J. Condensed Matter Nucl. Sci. 19 (2021) 167–185

Research Article

Cavitation and Radio Frequency Stimulation of Water to Alpha Particle Production

Roger Sherman Stringham*

Firstgate, 4124 Kapuna Rd., Kauai, HI, 96754, USA

Abstract

Radio frequency (RF) cavitation of water using an RF amplifier has been under development for the last five years as a 2 MHz producer of high concentrations of small cavitation bubbles collapsing in water. There is little doubt that helium atoms were produced from RF at 2 MHz during cavitation of both DOD and HOH. The path for D to He looked much simpler, so the effort was placed there as the path for H to He appeared to be too complex. Measuring and finding He produced in a vacuum tight reactor with no air leaks where mass spectral (MS) system analyses numbers would be disturbed. The only He to deal with was in the reactor's pressurizing tank of Ar and that value of 0.10 ppm was subtracted from all measurements. Two systems were analyzed. In one, HOH and Cu produced 1.7 W for 45 min. and in system two, DOD and Pd/6% Ag produced a burst of 6 W for 250 s. A comparison was made between cavitation and muon systems. A very slow rate muon system also produced He. The two impulse systems, I_{sw} and I_{μ}, were compared, and the cavitating system's impulse was 60 times greater than the muon system. The two systems differ. The cavitation system was explosive, and the muon system was implosive. The cavitation system was fueled by 15.5 eV of energy, and the muon system was fueled by $23.8\times10^{+6}$ eV of energy. The cavitation system reaction rate was 1.6×10^{-15} s, and the muon system was 10^{-6} s. From this point of view the cavitation system looked more favorable than the muon system for He production.
 ISSN 2227-3123

Keywords: Cavitation resonance, Free electrons, Mass spectrum, MC clustered deuterons, Radio frequency, Target foils, Timeframe

1. Introduction

1.1. The mesoscale of atoms of various particles in maso clusters (MC)

The mesoscale is applied to atoms or ions that maintain some degree of coherence during their short lifetime. As one looks into meso clusters (MC) of deuterons injected into a free electron environment of a target foil (TF) surface at a temperature initially at ∼5000 K the environment is too hot for recombination and in MC containment. The probability of an electron combining with an MC deuteron remains low in the 50-fs timeframe. Not until the temperature drops to a suggested value of ∼2500 K will D* form and produce an SW capable of producing an alpha. The philosophy here was to show the SW system, when compared to a known He producing muon system appears to be more likely than

*E-mail: rogerssbiz@gmail.com.

 ISSN 2227-3123

the muon system to produce an alpha particle (He) and in the experiments He^4. The activity during the implantation of D+ into the target foil, TF, lattice was the initial process followed by the 50 fs meso cluster, MC, that produced one alpha for each event. And it was the accumulation of these events that were measured by mass spectrum to give the number of He^4 atoms (the alpha particle production).

The philosophy here was to show the SW system, when compared to a known He producing muon system appears to be more likely than the muon system to produce an alpha particle (He) and in the experiments He^4. The activity during the implantation of D^+ into the target foil, TF, lattice was the initial process followed by the 50 fs meso cluster, MC, that produced one alpha for each event. And it was the accumulation of these events that were measured by mass spectrum to give the number of He^4 atoms (the alpha particle production).

1.2. Sonofusion and RF

The RF system is a non-obvious extension of Sonofusion, where a replacement of the oscillator with an RF input by a linear RF amplifier (1.5–10 MHz) at 2 MHz, where the piezo functions as an antenna. The amplifier was tuned to a minimum RF reflection and maximum admittance with a standing wave ratio (SWR) close to 1.00, indicating 100% signal transmitted. There were other tuning methods that can be utilized: oscilloscope voltage, the frequency resonance, the visual D_2O surface movement, and the oscilloscope overtones. Some new discoveries about the cavitating system have been made during this 2-year experimental campaign: (1) there was more than one vibrating surface and (2) the fundamental vibration may make some large contributions to the resonant bubble population via overtones.

The RF cavitation shows a cavitating producing sonoluminescence system measured by MPPC Hamamatsu photon devices (in a separate experiment). At R_o an adiabatic collapse to R_f occurs. A sonoluminescence red pulse peak, SL, of photons lasting for less than 10% of the MHz cycle time, 5×10^{-7} s, is coupled to the RF input, black line, during that one cycle. Each bubble grows from the low-pressure $R_{i,}$ green, gaining mass of D_2O vapors. The plasma, red star, implants deuterons into an MC on the surface of active area of 50 mm^2 TF surface

1.3. Monitoring the RF frequency

Cavitation has a varied history and was first patented in 1960 by Hugh G. Flynn 1982 [2] and later by S. Putterman 1994 [3] and R. Stringham 1992 [4]. The path used by this author moved from frequencies of 20 kHz in 1989 to 2 MHz 2016 and relies on the mechanism having the same cavitation energetics as the low frequency, 20 kHz, systems. Figure 1 shows at top that the cavitation pulse is a short burst of energy lasting less than 10% of one cycle. The pulses narrow as the frequency increases. We have many data sheets showing these photon pulses coupled to frequency input. There is no activity during the rest of the cycle [5], only cooling. These measurements were made during 1600 MHz using a cavitation oscillator. This figure indicates that at 10 times the frequency there would be no problem with the mechanics completing the cavitation cycle. To clarify the acoustics a plastic strip 0.8 cm × 4.0 cm, of PVDF film was fastened outside surface of the reactor placed opposite the piezo PZT disk, and audio output was continuously viewed on the scope [5]. The output showed complex beat patterns of 17 per cycles for each input cycle. Its sensitivity reached into the high gigahertz range.

Experimentally, RF interference was a major concern that accompanied all measurements made while the RF system was running. To minimize RF interference on thermocouple measurements, a duty cycle was introduced of 30 s on and 5 s off that provided an adequate time window for credible measurements of temperature; this feature was built into the calorimetry of both the running RF mode and calibration mode.

Two years of RF practice runs with H_2O suggested that enough knowledge was in place to do controlled runs with D_2O. There was a different philosophy with the new RF reactor. The reactor was no longer a small polycarbonate 50 g reactor with a 1 cm^3 of actively cavitating D_2O volume with 1 ml/s circulation rate [5]. The cavitation was at the bottom of a 5-inch column of water and the kept cool by a circulation process (see Fig. 4A).

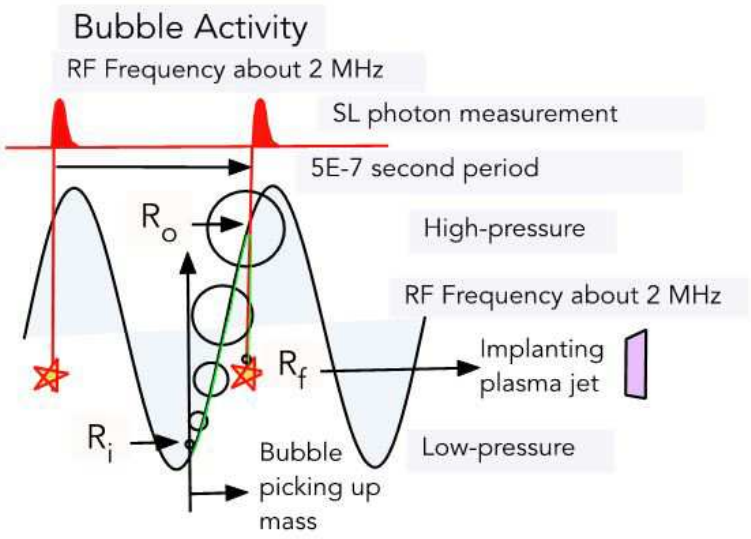

Figure 1. Shows the RF cavitation 2 MHz bubble collapse and its implantation into the nearby TF lattice. This is followed by the deuterium ions capture of an electron [1] and alpha production.

1.4. The SEM of MHz TF cluster 50 nm radius ejecta sites

Figure 2A. 1.6 MHz input. This shows the surface of the exposed TF and a cluster of small crater events in cavitating D_2O. (2B) shows a 1 μm^2 detail, red box. Most of the ejecta are single events with 15% that are darker considered the result of the ejecta with twice the energy or two events. The calculated lattice volume of a single ejecta event was equivalent to one alpha event, 4×10^{-12} J. The density of events is very high and if spread out over the foil surface was about one/million surface atoms that would be about 1/30 times as dense. If the He^4 ejecta sites in the detail were distributed over the active 50 mm^2 surface area there would be 1 ejecta sight in Fig. 2B detail. In other words, the cluster effect would be unnoticed. SEM photos by Jane Wheeler, Evans Lab., Sunnyvale, CA [6].

1.5. The RF acrylic reactor

The RF reactor consisted of a 2-inch diameter Acrylic tube with 0.25-inch wall and with placement for adjustable spacing and sealing gaskets for the PZT 20 mm disk piezo at the bottom of the reactor. The utilities enter through the 3-inch diameter 1-inch plate that was O-ring sealed to 3/4-inch thick and the 3-inch diameter plate. The two Acrylic plates were bolted together. (Some of the utilities were temperature, pressure, Ar gas, vacuum access, calibration heater, and gas sample vessels.) The system was run attached to the vacuum line and could be filled and run making calibrated ΔT measurements via a 5 s off mode of the duty cycle. The calorimetry involved the flow of coolant water through two identical copper coils. One coil in the reactor cavitating water, and the other coil in the 3.5 L heat sink water reservoir (see Fig. 4A). The RF reactor was run at RT of $\sim$24°C and ΔT never reached above of 10°C. The water circulation was by an FMI Inc. displacement pump at flow rate of 1.08 $\pm$0.02 cm^3/s. The objective was to collect the gases from the that Ar saturated volume and measure its He^4 content in ppm.

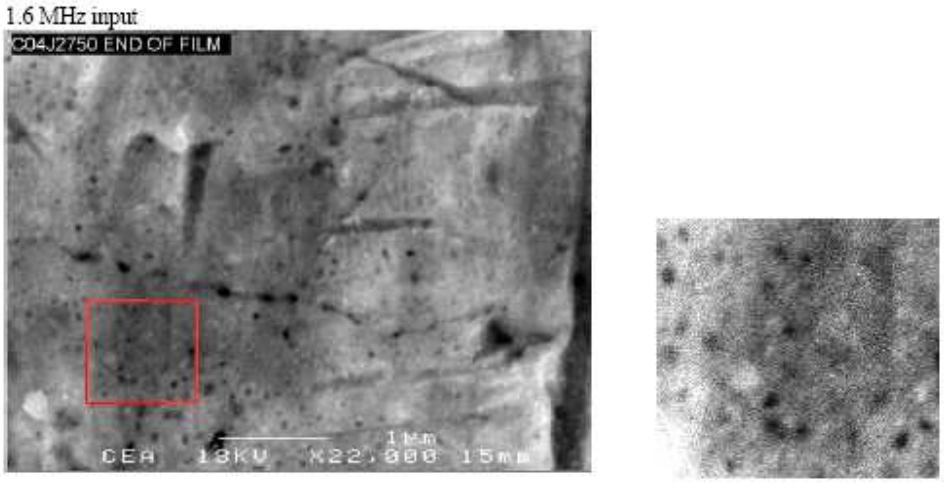

Figure 2. Shows Pd foil with many 100 nm diameter craters from cavitation and a detail to the right. These size and larger cavities are found in BCC lattice target foils.

1.6. Potential He^4 and Ar gas measuring problems in Acrylic RF reactor

The mass spectrum measurements showed the presence of small hydrocarbon molecules associated with the Acrylic reactor. Small amounts of a transparent viscous substance that was found on the reactor copper coil after a Run and dried to clear film could explain MS anomalies. These looked like an air leak in the reactor run in MS analysis. About a year later the confusion was neatly cleaned up. During the cavitation the reactor interior was dissolving from the Acrylic reactor surface and the low molecular weight of fragments were carried into the gas phase of the sample. The MS counted these unexpected fragments as air. But on further examination they were Acrylic fragments and thus reduce He^4 measured. The amount of He^4 in the dissolved Acrylic during its manufacture was calculated to be 10 times less than detected if the dissolved Acrylic was less than 1 cm^3 of the reactor inner surface.

1.7. The 2-year test period and the phantom temperature bursts (PTB)

During testing of the Acrylic RF reactor that were run in about 80 ml H_2O, it was a common experience to see superimposed on the H_2O heating curve an abrupt increase in T for a few cycles, which then collapsed back to the heating curve as the duty cycle was continuously removing heat to the 3.5 L coolant reservoir as the RF apparatus was in the running mode. These phantom temperature bursts (PTB) [7], events occurred regularly some lasting for an hour and others for a few minutes. The PTB amplitude often doubled and sometimes quadrupled the heating curve that always remained the same. The measurements were in Acrylic tubes the same size as the machined vacuum RF reactor. No MS measurements were made of gases from these early experiments as they were saturated by the air's natural content of He^4. These same PTB were found running the RF reactor using the same duty cycle.

Figure 3. Shows the polycarbonate reactor with utilities entering from the top for the RF reactor passing into the cavitating Ar saturated DOD. One of the two copper coils is shown in the RF reactor where coolant water was circulated cooling the reactor operation.

2. Experimental

2.1. Experimental setup

The duty cycle was used in all run and calibration modes. Two years of RF practice runs with H_2O suggested that enough knowledge was in place to do controlled runs with D_2O.

As noted, the old reactor was a small polycarbonate 50 g reactor with a 1 cm^3 of actively cavitating D_2O. The RF system uses a 5 $\times$1.5-inch column and diameter of D_2O while keeping the static D_2O close to steady-state temperature by using the second 16 loop Cu coil submerged in a 3.5 L tank of coolant water as a heat exchanger. The coils were 1/8-inch OD and about 4 inch long. The setup required about 1000 s to reach heat input equilibrium. The D_2O, Fig. 4A, removes heat moving water coolant H_2O via an FMI displacement pump moving the coolant into the 3.5 L water reservoir through the #2 coil then back into the D_2O and reactor coil, cycling at a flow rate of 1.08 ml/s. There the heat was collected in the 3.5 L insulated tank that moderates the running temperature of the reactor bringing a more efficient lower temperature cavitation. Figure 4B shows the TF placement in the reactor where its surface craters were produced on the TF. This for the FCC TF lattice. A number of 20 mm$\times$0.002-inch gaskets of Neoprene and Teflon were used to adjust the geometry piezo and TF as well as seal the containment in the vacuum tight reactor.

The implant of the cavitation bubble collapse, the jet plasma squeezed by the EM field of the sheath electrons, is where the sheath's outer electrons implant first. Followed by hot deuterons. These particles maintain their charge separation becoming the 50 fs MCs in the surface of the TF lattice. The timeline indicates the impulse path to products and compares SW gain of an electron and gain of volume of space in forming D^*. Compared to muon's loss of electron from the D_2 molecule collapsing to the very small ddμ . It loses an electron, and loses that volume of space associated

with the volume of D_2. $D_2 + \mu \rightarrow dd\mu + e^-$. The difference of the two systems, SW is gaining an electron and gaining volume (space) and the D_2 system is losing an electron and losing space (see Fig. 1). An interesting comparison of the same alpha products by viewing impulse of I_{SW} and $I_{\mu-}$ and the process size changes. I_{sw} has a low energy of α formation of 15.5 eV and very fast rate of formation of 6×10^{-15} s. As there was an electron capture and there was a gain in product size $2D^+ \rightarrow \alpha^+$. I_μ has a high energy of α formation of 24.8 MeV and a slow rate of 10^{-6} s. There is an electron loss and a size change of $D_2 \rightarrow dd\mu$. This was shown in Figs. 4A and 3B.

2.2. The collection of data during the RF experiments (35 s duty cycle)

The RF used in these experiments prevents the direct measurement ΔT with thermocouples as the wires act as antenna and no longer are sensitive to temperature. To remove this problem, the temperature measurements are made during a 5 s off mode (a 5 s off period) coupled to a 30 s on mode (RF heat period). This on off duty cycle allows for a good temperature measure during the progression of the heating curve with no Radio Frequency Interference (RFI). The duty cycle is on all the time during the run mode and calibration mode with a cyclic circuit breaker to the input power. It has been on for years for that circuit. It gives me a clear set of data that does not require any thought to data changes during the run and calibration modes. Each 35 s cycle data joins the next 35 s allowing for a seamless ΔT data production.

3. RF Water Experiments

RF system and piezo geometry. Figure 4A is the reactor setup. It runs at lower temperatures as the D_2O or H_2O RF reactor is coupled with a 3.5 L with 1 of the 2 Cu coils for heat removal from the running mode of the cavitation circulation system. The coolant, light blue, is circulated through the heated system giving up heat to the 3.5 L coolant reservoir that is replaced by cool water. The FMI pump continuously circulated coolant water at a rate of 1.08 ± 2 ml/s for a year. The ΔT, T_{out}-T_{in}, after 1000 s reaches steady state. Any positive deviation of the heating curve was excess heat Q_x. During the calibration mode there was in the center a 10 W stainless-steel clad coiled heating element, red, from ARI that substitutes for RF linear amplitude amplifier input. At heat input, equilibrium heating, and cooling curves, running and calibration mode should always be data sound with no excursions. Figure 4B the Acrylic reactor was sealed 20 mm ring gaskets of neoprene and Teflon that were adjusted and spaced to seal the reactor vacuum tight and a good piezo TF geometry.

3.1. Old runs in air with no MS

The examples below, Fig. 5A and B, of the old PTB, from several years ago that were disturbing because they were observed in both light and heavy RF cavitating water and Cu TFs. This important subject will be found in Section 4.5. The older initial RF experiments of 2016–2017 contributed to the mastering of this unknown PTB [7] effect that was

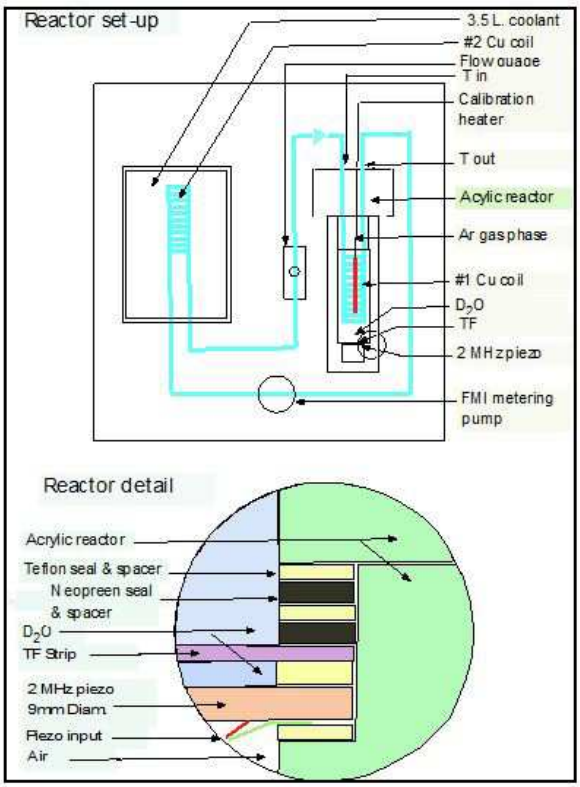

Figure 4. (A) shows the RF circulation system flowing through the two copper coils, blue. One coil removes heat from the DOD in the cavitating RF reactor the other returns cool water to the RF reactor flow system at a rate 1.02 ml/s. (B) shows a detail of the 2MHZ piezo and the target foil geometry and spacing ring gaskets that seal and clamp the piezo and target foil.

so prevalent in the collected data. A learning curve where one could build and add more data and become familiar to something that was quite foreign.

3.2. Two years of PTB work in air using H_2O

The RF system with many experiments that show through interpretation the explanation of phantom temperature bursts, PTB in early RF experiments in H_2O. The comparison of light and heavy water was to use light water as a blank. Unfortunately, the early light water experiments produced these PTB. This was just a testing system. From the perspective of a few months earlier it became much clearer. For 2 years it was a struggle having these PTB with all experiments. The author had two reactors machined for the MS and tritium analysis never knowing the PTB was exactly what the author was looking for. It was not until 2020 that the author realized it was what we were looking for, but the data was only good for heat generation. He^4 MS measurements for air experiments would be useless.

3.3. The Lucite reactor

The new RF reactor was machined by Hans Huber from a 6-inch Acrylic tube, having a 2-inch diameter OD with quarter-inch walls. A one-inch thick by 3-inch diameter disk top was provided, where all the utility and measuring pass-throughs were positioned, except for the RF piezo input placed at the tube bottom with the PVDF audio pickup. A 1/8-inch diameter copper cooling coil of 16 turns was submerged in the static D_2O. This coil moved coolant water at a measured rate of $1\pm$ 0.02 ml/s (see Fig. 4A). The purpose was to remove heat, keeping the D_2O at a low constant temperature. Equilibrium was reached after running about 1000 s. The water coolant flows from Cu coil # 1 through a closed loop to an equivalent second identical copper coil submerged in 3.5-liter coolant water reservoir. The RF system gathered data using a video camera correlating the many parameters, using the sweep second of the clock to point out and store any running changes during an experimental process. The RF geometry and methods were very different from the 50-g polycarbonate circulating D_2O liquid system [5].

3.4. How it worked and the PTB

In older developing technology the calculations for the PTB were thought to be the evidence of excess energy in joules over the $\Delta(T_{\rm out}$-$T_{\rm in})$ and was converted to MeV. We needed to find a correlation between the PTB heat, in MeV, and the suspected MS measured atoms He^4 in ppm. The data can be keyed to the calculated number of Ar atoms in the gas phase above the surface of the cavitating water. Both Ar and He^4 are noble gases and have the same physical properties and will have the same distribution tendencies such as low solubility in water. The cavitating water will tend to push Ar and He^4 out into the gas phase, Ar, and also helped by their already insoluble characteristics, it will push more of these atoms into the gas phase of the reactor. The volume of the gas phase becomes an important part of the He^4 MS analysis measured in ppm 50 ml volume. Any He^4 that was measured by MS was related the total Ar atoms in the gas phase of the reactor. Knowing Avogadro's relationship we calculate the number of Ar atoms gas phase volume and knowing the measured ppm of He^4 it was transferred let us estimate the number of atoms of He^4 produced (one must subtract the ppm He^4 impurity in the Ar that pressurized the experiment; it was 0.10 ± 0.02 ppm).

3.5. Figures 5A, 5B, 6A and 6B

The old work shown in Fig. 5A and B was done in an air environment show only the PTB. The power input was increased through the 2-year data collection period. Initially there was no MS or tritium analyses in the experiments. Later experiments showed:

A. Old RF test runs in air with no expectation pf measuring He^4. A 2 year period was the learning curve for thee tests, The PTB were initially considered artifacts. All test runs were done H_2O and used the 35 s duty cycle. These are two typical runs. (B) Top curve- A 40 W RF acoustic input in a low mass air reactor within an interrupted cooling curve. The PTB are random on top of the RF input. Bottom curve- A 40 watt RF acoustic input just like the top curve. Figure showing the random nature of the PTB. There were dozens of these temperature excursions

For the 1.5 inch diameter Acrylic tubular reactor with RF, cavitating H_2O was the run mode, and the 10 Ω resistance from RFI, was adjusted for with the on-off duty cycle. The reactor clear space above the liquid surface is the confining space of the of gas phase volume of about 40 and 36 cm^3 volumes Ar and He^4, that was measured by MS analyses by Malcolm Fowler at MISI Lab. mailed to him in 50 cm^3 Pyrex sampling vessels. This collected gas phase above the cavitating water that was removed from the reactor within 10 min of turning off the calibration mode at the end of the experiment. The He^4 and Ar were not very soluble in water. The Ar tank of very high purity was measured by the same MS as the RF samples. The source of He^4 in the tank of Ar used in RF runs in the amount of 0.10 ppm must be subtracted from all the MS measurements.

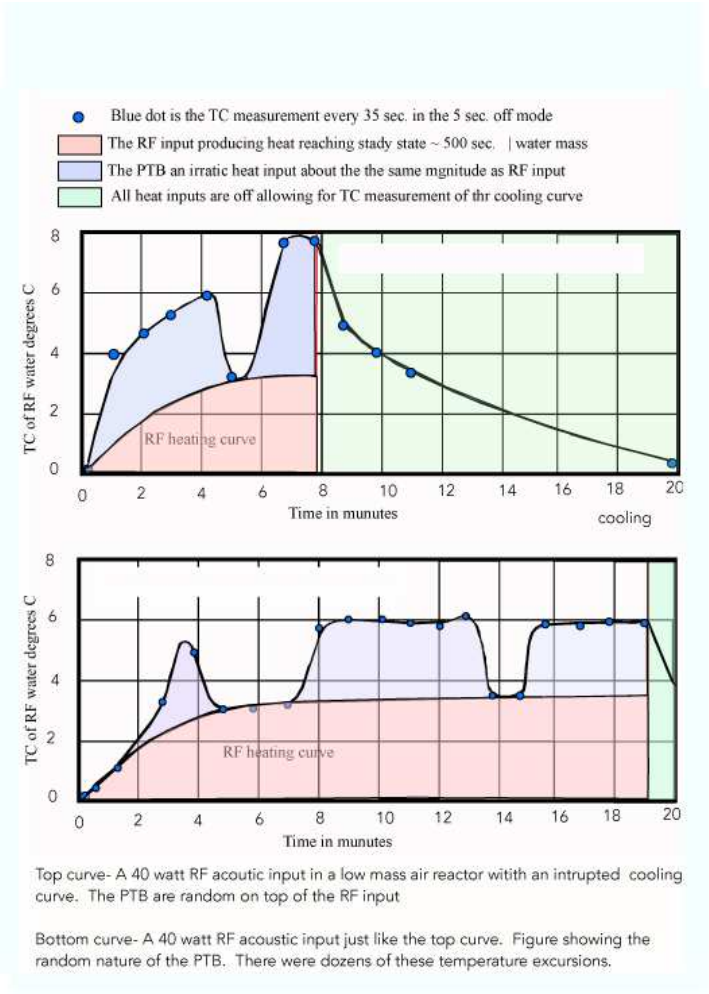

Figure 5. (A) and (B) were two examples of the phantom temperature burst, PTB, data showing heat from the cavitation input and the PTB data added to it.

Figure 5A and B was typical of many RF runs from several years ago with light water and with the random production of ΔT PTB heating. There was no apparent cause for these events to occur, but they were unique for the RF systems. The rose color of RF heating reached a steady state ΔT in about 500 s. (In later work with the more massive and robust machined Lucite reactor the equilibrium time was doubled to about 1000 s.) The ΔT amplitude for the PTB was significant and easily measured above the RF input. Also, some of the heat from the PTB added heat continually in H_2O systems as shown in Fig. 5A, with a slow rise in ΔT. A steady state will only be found in the calibration mode.

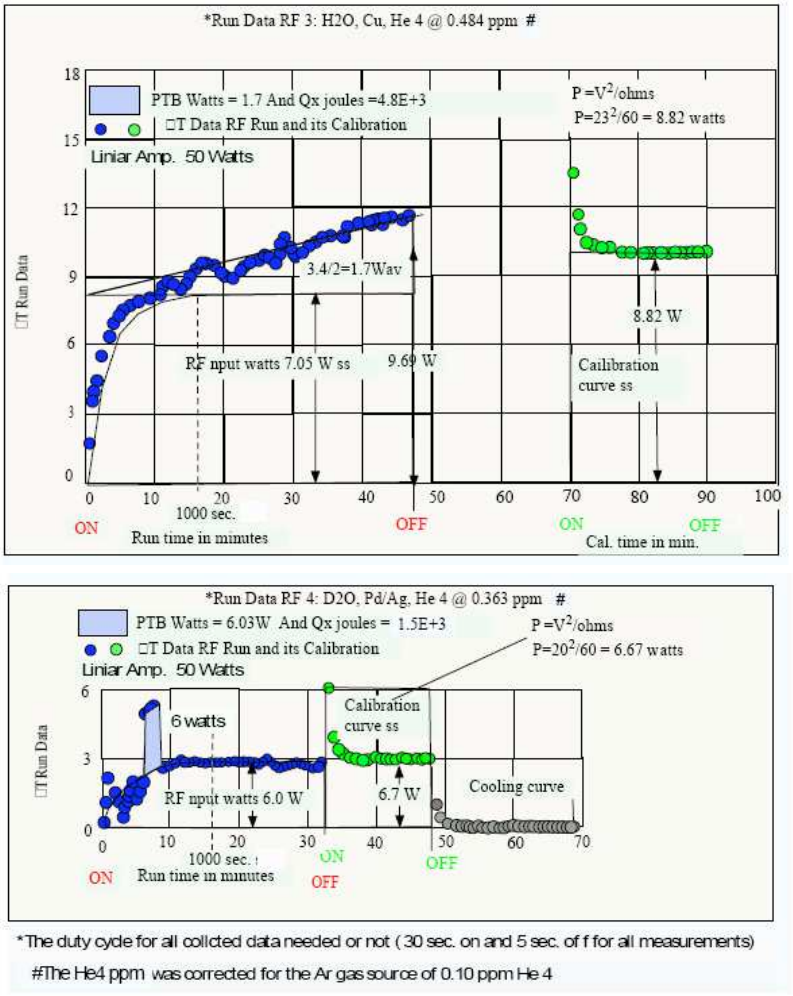

Figure 6. (6A). RF #3, 4/26/2018, H_2O, 47 min, He^4 .484 ppm, TF Cu. 127 μ m thick – MS found $2.356\times 10^{+15}$ He^4 atoms. (6B). RF#4, 5/07/2018-, D_2O, 33 min, He^4. 0.326 ppm, TF Pd/Ag. 100 μ m thick - $176\times 10^{+14}$ He^4 atoms.

3.6. Figures 6A and 6B

Figure 6A and B was in the vacuum RF reactor that produced the same ΔT PTB events. There was no apparent cause for these events to occur, but they were unique for the RF systems. The rose color of RF heating reached an equilibrium state ΔT in about 1000 s. It was not unusual for the PTB to equal to the RF input. Also, some of the heat from the PTB added heat continually in H_2O systems as shown in Fig. 6A and produced a slow rise in ΔT. A steady state will only be found in the 60 Ω calibration heater mode.

The later vacuum RF He^4 experiments in Fig. 6A and B of the PTB, show the He^4 measured by Malcolm Fowler MS analysis in his lab. Samples of the RF gases sent to Thomas Claytor's laboratory (HML, in Los Alamos NM) were examined for tritium. If tritium was present, it was below background.

3.7. New data with 50-W linear amplifier and MS of He^4 collected gases

Figure 6A and B shows two RF recent runs that had the MS measurement for He with light and heavy water with the random production of ΔT PTB heating. These were both run with the 50-W linear acoustic amplifier and a PVDF acoustic pick-up. The temperature measured during the 5 s off mode showed a rapid T cooling during the 5 s measurement but not enough to alter the ΔT measurement. The PTB with H_2O, Fig. 6A, RF3; H_2OCu had a continuous configuration, where RF4; D_2O Pd/Ag had more of a spike PTB, Fig. 6B. If you spread out the first 6 min, it appears quite spiky. We only looked at the big spikes at 7 min into the run and ran for about 250 s. The cooling curve in the runs tends to conform to regular cooling activity as do Fig. 5A and B where H_2O cooling curve and is reasonable but not complete. The rise in ΔT is assumed for the entire mass of water, where the activity of the cavitating water was measured at the thermocouple, TC, as coolant exits and enters the copper coil heat exchanger system, Fig. 4A, in the RF cavitating Ar saturated water (D_2O and H_2O). While running the ΔT was never more than 10°C. It is advantageous to keep the running ΔT less 10°C for two reasons. (1) Running cool at a base of 24°C the Δ10°C is good for cavitation; (2) heat loss through the 1/4-inch Acrylic RF reactor wall was kept to a minimum with the low ΔT. It was not until this run that the clear viscus liquid was first observed.

3.8. RF water cavitation, Fig. 6A and B, measurements for He^4 and tritium

Sample RF#3 H_2O Cu TF, in Fig. 6A: The gas pressure Ar was 1.1 atm and temperature 309 K in RF reactor Ar gas volume of 36 cm^3 that was over the cavitating H_2O where 50 ml gas volumes sent for MS and tritium measurements. The ppm of measured He^4, 0.363–0.1 = 0.236 ppm will remain the same in the reactor and the sample volume. To make the conversion simple, find the number of Ar atoms over the cavitating D_2O (reactor gas volume of 36 cm^3). The moles of Ar in reactor volume are, 36 cm^3/22 400 cm^3 (STP) =1.616×10^{-2} mol. Correct for $T/P = 1.13/1.1 = 1.03$. find how many Ar atoms in the gas phase volume of reactor. $1.03{*}{\times}1.616{\times}10^{-2}{\times}6.0226{\times}10^{+23} = 9.976{\times}10^{+21}$ Ar atoms. And MS measured 0.263 6×10^{-6} × He^4 atoms and then multiply by the number of Ar atoms, $9.976\times10^{+21}$, yields the number of He^4 atoms $2.356\times10^{+15}$ atoms. For the 2820 s run energy in joules = 4800 J convert to eV =$36\times 10^{+22}$ eV and eV/He^4 atom is $2.356\times10^{+15}/(36\times 10^{+22}) = He^4/eV = 7.86\times10^{+6}$ MeV/He^4.

Sample RF#4 D_2O Pd/Ag TF in Fig. 6B: Measurements for 4He was 0.484 ppm where 0.10 ppm was subtracted leaving 0.384 ppm MS measurement produced on the surface of Pd/Ag target foil. Whether any He^4 was left in the TF is unknown (pp). To make the conversion simple, we find the number of Ar atoms over the cavitating D_2O (reactor gas volume of 40 cm^3). The moles of Ar in reactor volume are, 40 cm^3/22400 cm^3 (STP)= 1.796×10^{-3}. Correct for $T/P = 1.13/1.1 = 1.03$. To find how many Ar atoms are in the gas phase of reactor: $1.03\times 1.796\times10^{-3}\times 6.0226\times 10^{+23} = 1.016\times10^{+21}$ Ar atoms, therefore at $0.3846\times10^{-6} \times1.016\times10^{+21} = 4.25{+}14$ He^4 atoms. The energy in joules = 1500. Convert to eV =$9.366\times10^{+21}$ eV and eV/He^4 atom is $9.366\times10^{+21}/(4.25{+}14)$ ev/He^4 atoms =$2.206\times10^{+7}$ eV/He^4 atom.

3.9. The results of the MS He^4 measurements

The error in these He^4 measurements is estimated at ± 60% that results from the complex nature of the gas handling process and the MS measurement itself of ± 10%. The process at the reactor end and the MS end coupled with the discovery of new developments of parallel processes going on were such that I did not realize the problem at the time, and were resolved later. It was months after stopping RF runs that the picture began to emerge as to what was going on. A clear viscous material was forming in the reactor that was present in the debris of the experiment and it gradually became clear. When this material dried it became clear brittle film like Acrylic. The new reactor and the new 50 W and high-powered Linear Amplifier from HD Communications replaced the older 20- and 40-W Linear Amplifiers. The new system was actively dissolving and digesting the inside surface of the Acrylic RF reactor.

Fragments from the polymer (CH_2, CH_2O, —) were showing up in the MS SRS RGA-100, 1-100 amu mass spectrum of Malcom's measurements [9] and points to how successful the analyses were. This does not change the RF reactor He^4 measurements, but it removes the argument of an air leak somewhere. However, it introduces is a possible source of He^4 in the surface material cleaned from the reactor. But it was calculated and found to be no problem at less than 1% of 0.010 ppm.

The final step in the measurement of He^4 was after the traps and filters MS flow of atoms of the species of *least column residence time* would be He^3 and He^4 moving in the packed columns at LN temperatures. The first atoms through, the fastest atoms, would be He^3 then He^4. These atoms would have the least residence time through getters in the column which remove protons and their isomers. These were directed to an Alcatel ASM-110 Leak Detector, with a sensor that was monitored by TDS-744A digital scope. This short retention time would be the proof of the atom species [8].

4. Impulse a Change in Momentum

4.1. Compare to known He^4 producing system (muon)

It is important to compare the SW system to a He^4 producing muon system [9]. The SW system squeezes the MC deuterons when the first free electron combines with deuteron forming D* atom that combines with a D^+ in the debris of the MC forming the alpha. In the comparison at the atomic scale of the MC and the muon impulse, I_{MC} and $I_{\mu-}$, where the MC SW rate, in the MC, is $1.67\times10^{-15}\mathrm{s}^{-1}$ that produces one helium atom and the muon system produces a hydrogen atom (see Fig. 6A and B). The production of He^4 in along muon paths can be at rates slower than the half life of the muon, 2.2×10^{-6} s. The I_{sw} and I_{μ} are very different in space time. That will be discussed in a future paper.

4.2. The mechanics are treated as atomic level SW and muon impulses

The impulse, ΔP, the change in momentum over a short time period were compared, I_{SW} and I_{μ}. When using the term μ it refers to μ^-. The two systems that produce He^4, one being an SW with D^+ the other being μ with D_2 have rates that differ by 10^{-9} s^{-1}. The impulse experiments are measured in kg m/s (mv). $\Delta P = I = F\Delta t \sim md/t$. The impulse rate of 10^6 s^{-1} is almost the same size as its half-life but still produces He^4 and is compared to SW rate of 1.6×10^{-15} s^{-1}. The He^4 SW production looks like it might be a good path choice for alpha production. Another path choice is the Lawandy's image attractive force between like charges applied to deuterons [10].

4.3. The impulse (explosion and implosion) (also bottom page 2). Fig. 6B #4RF D_2O

Table 1. The impulse.

I (impulse	Mass (kg)	Energy (eV)	d (m)	Time period	Impulse (kg× m/s)	Log time period (s)
I_{sw}	6.68×10^{-27}	15.5	5×10^{-11}	6×10^{-15}	0.207	–14.22
I_{μ}	6.87×10^{-27}	$24\times10^{+6}$	5×10^{-11}	10^{-6}	0.0033	–6.00

4.4. Rates and time period are reciprocal

The first order rates for various paths that relate to I_{sw} and I_{μ} systems and produce products might be as slow as the 2.2×10^{-6} s half-life of the muon. For the first order reaction rates used here the reaction rate is 1/time period. The

time period for the $I_{\rm sw}$ is 6×10^{-15} s and is associated with the time of one revolution of an electron around the D atom [1]. The time period for the I_{μ} is 10^{-6} s and is associated with the time of the slowest muon system that produces a helium atom [9]. It produces He, and compared to the $I_{\rm sw}$ system that was 6×10^{-15}s. it is 10^{+9} slower.

5. Discussion

This discussion is about FCC surfaces of TF Pd, Ag, Ni, Cu that have ejecta that include alpha production.

5.1. Temperature measurements need a duty cycle

The RF produced an environment that makes it impossible to take TC measurements during running conditions of RF experiments. So, an *off–on* duty cycle was installed for all measurements for the running and calibration modes, and this makes it possible to make thermocouple measurements during the 5 s off period for each 35 s cycle.

During the 5 s off period the system goes into a cooling curve where the rate of cooling is at a maximum. There are a number of temperature points measured so the first points in the 5 s off mode best represent the ΔT of the cooling mode maximum temperature for that data point. In the heat equilibrium of the running mode and steady state of the calibration mode every data point represents a slight saw tooth path over the total a thirty-minute run. This makes the temperature read a bit lower than reality and has little effect on the systems data collection.

5.2. The average free electron velocity at 10 K

From plasma physics the average free electron v $\sim 6\times10^{+5}$ m/s. (8 kT/(π m))$\cdot^5$ m/s. This indicates that there is no potential problem with free electrons at 10 K are far from interference by relativity effects of impulse measurements due to high velocities involved in the produced impulse momentum measurement and calculations [6].

5.3. The more recent MS measurements show H_2O cavitation produces He^4

Showing that H_2O in the identical system was planned as standard and not as an active He^4 producer. It was using H_2O starting in 2017 that the anomalous PTB were noticed and were common to the point of being ignored and a nuisance. The author learned to live with it unexplained and the author was looking for He^4 from the D_2O system. The first years of work showed a constant presence of the PTBs. These events were never reproducible and sometimes long duration, or as short as a minute, and variable amplitudes (several times the input ΔT). But the PTB also showed up in the more sophisticated experiments, under vacuum conditions, where low amounts of He^4 could be measured as a product. Such as runs like RF#3 Cu H_2O and RF#4 Pd/Ag D_2O where He^4 was measured. This forced a reevaluation of a mindset that the old the data, $\sim$100 runs, that were produced for several years as practice in air in water systems were not artifacts but a real ΔT. Where the systems were not limited bosonic systems but were more general and included fermion and mixed systems as well. Everything now must include the three hydrogen isotopes. The only element that possess this violent space change in the transformation from the ion to its atom. The main line will follow D^+ activity but also should be adapted to H^+ and T^+. For instance, the MC of H^+ could produce D^* and the MC of T^+ could produce $T^+ + H_2O \rightarrow$ alpha $+ HO^+$. T^+ has not been found above background in the measurements from Claytor's HMT lab.

5.4. SEM measured crater at TF power cut-off

A cavitation produced crater is a single event that is near the smallest produced and in the size spectrum of produced in the spectrum of craters, as suggested from a number of SEM photos. There is not much evidence of smaller craters

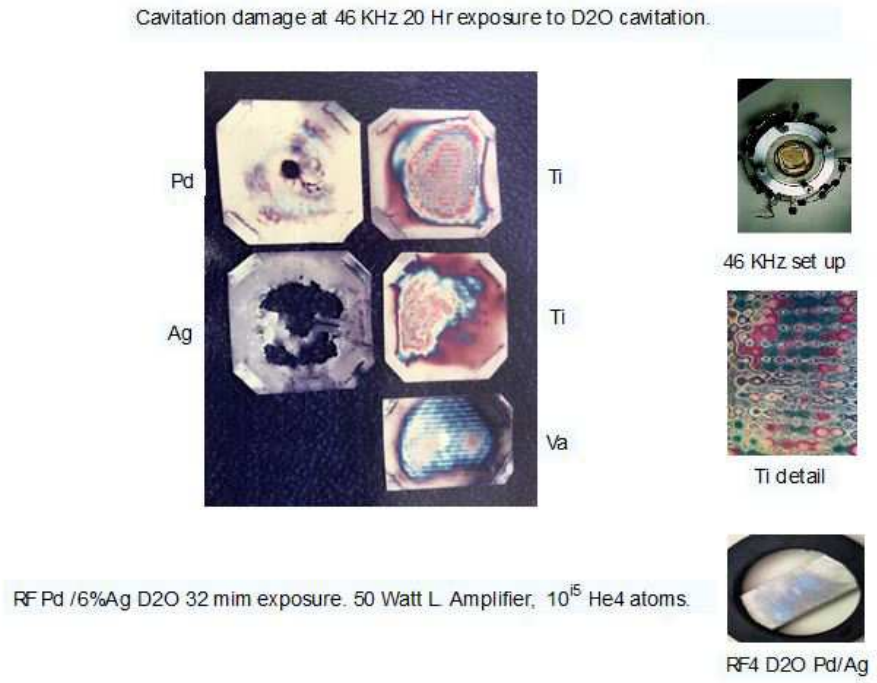

Figure 7. Shows some interesting target foils exposed to cavitation and their standing wave surface patterns that were captured during the cavitation process. Some intensities and small craters were from too long or energetic exposures. The photos to the left were at 20 kHz exposed for 20 h. Two foils upper right at 46 kHz and lower left was exposed at 1.6 MHz. All TFs were about100 μm thick.

and the author speculate they are the result of damaged craters from earlier events. There was a continuous turnover in the active TF surface. The TF surface is reworked with each cycle. At high frequencies such as 2000 kHz, small 50-nm radius craters are evolving at a steady rate during the cavitation process. New craters are continually replacing the old. SEM photos reveal the last generation of the crater production. The TF surface continues to evolve until the power is turned off. Some smaller cavities are from damaged craters from earlier impacts were found. The SEM of removed TF from cavitation exposure shows the latest version TF crater surface that is frozen and can be studied further when the instrumentation is available. There are a hundred of these foils in storage.

5.5. Cavitation damage to TF surfaces from 20 kHz to 2 MHz and their standing wave patterns

Figure 7 shows the colorful exposed TF of the past that were made at 46 kHz D_2O cavitation exposure in 1995 of both types of lattice [15], FCC and BCC. The coloration in FCC TFs was not as gaudy and the lattice damage was more severe, as shown on the far right. Note the clarity of the detail in the Ti foil. The standing wave is about 2 mm those pointed to a 2 MHz resonance system for future experiments. The gap distance between the piezo and TF. The input frequency should be about 1/4 wavelength of the resonance of Ti TF.

The RF D_2O Pd/6%Ag experiment shows a purple reddish exposed surface that produced $4\times\mathbf{10}^{+14}$ atoms of He^4 in 250 s, 6 W.

The cavitation damage to the TF surface is reduced by increasing the cavitation frequency but keeping the bubble collapsing mechanisms and densities the same in the small bubble systems.

5.6. Temperature and the first D^* or H^* atom

There is some uncertainty in the of a cooling hydrogen plasma when the first D^*, Deuterium atom, appears. In the timeframe of 50 fs and a temperature of 5000 K cooling to $\sim$ 2500 K a D^+ will pick up a free electron becoming D^* atom ($D^+ + e^- \rightarrow D^* + SW$). In this process that occurs in the MC there is a very rapid change in volume $\sim 10^{+7}$ times in a time period of 6×10^{-15} s and an SW. The uncertainty of the event's occurrence in the MC during its 50-fs duration must adjust to the cooling temperatures for the first and only D^* atom formation. This was the production of the alpha product. The temperature of formation of D^* is not critical but leads to SW and the complete destruction of the MC in the spherical electron squeeze. The pure astronomical H at 7000 K and H^+ at 10,000 K and as it cools to 7000 K is 100% H^+ and 2800 K 100% H^*. These temperatures are easily changed to fit. As the timeframe shrinks to 50 fs and a very few particles, 100 or less, there was a 50% chance it will happen by temperature adjustment. And in an Ar gas environment temperature can be adjusted to meet the requirements of the SW production as collisions with Ar atoms reduces the temperature used in RF experiments where at 2800 K the hydrogen is normally 100% H^* [12,13]. But in the time frame 50 fs the temperatures were adjusted to fit. The system goes from 100% protons to 100% hydrogen atoms by just altering the temperature environment in 50 fs timeframe.

During the MC 50 fs cooling period the single event of a free electron in the MC of deuterons manages to complete the capture and formation of a D^* atom (a D^+ capturing an e-) producing a SW and an alpha that scatters the MC debris (α, D^+, DOOD, DO^+, —) in and on the FCC TF, surface. In the BCC the debris was the same (D+, DOOD, $DO^{+,}$ —) except there was no alpha [14].

5.7. The difference TF lattices (BCC and FCC)

An earlier paper showed in SEM photos that in TFs without ejecta sites, the MS measurements of He^4 showed it was locked in the TF lattice of Ti, a BCC lattice [14]. The TFs showing ejecta sites were of another lattice configuration, two Pd samples, were FCC Pd TF. These two samples showed many ejecta sites and surface damage in their SEM photos where He^4 was measured in the gas phase, but not in the lattice of melted target foils. This was consistent with the observations of all FCC TF from several years of experiments.

5.8. Old SEM photos of MHz cavitation of FCC TF show 50 nm craters

The left-hand side of Fig. 8 shows an SEM photo of an exposed target foil during experiments at Claytor's laboratory in Dec. 2016 showing results from a small 50 g cavitation reactor that was oscillator driven at 1600 MHz. Ar saturated D_2O was circulated at 1 cm^3/s Most of the experiments were the calorimetry measurements that were difficult to reduce. But this SEM data fits new experiments done at 2 MHz [8]. SEM photo by Yuval Avniel

5.9. Volume change

It is helpful to describe the deuterium system and applying what is described for the other hydrogen isotopes. They all have a tremendous dV/dt values, change in volume, when their ions combine with the free electrons. All produce an explosive increase in volume and was their mode for MC destruction and ejection of He^4 from the FCC lattice. There is more information in [5] about Ti TF. There were no ejecta sites observed in SEM photos of Ti BCC TF and their debris from their cavitation environment was from TiOx micro tubes. The BCC TF active surfaces were covered with

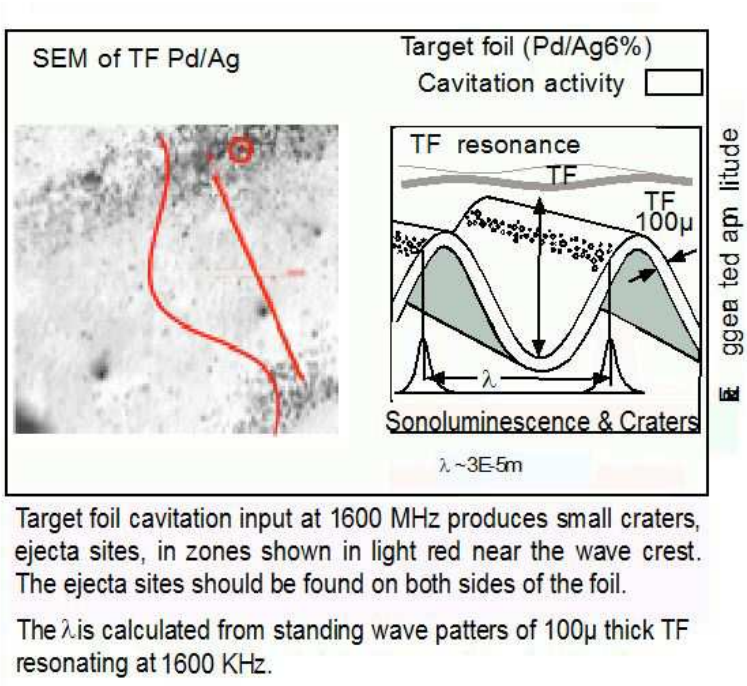

Figure 8. An SEM of a Pd TF exposed to 1.6 MHz and its interpretation. One can see the cavitation damage to the FCC lattice due to this exposure.

TiO_x in the form of fragile fragments of 1 μ m tubes that produce the exotic colored surface standing wave patterns. The debris of these is formed and what the SEM shows is the what was formed in the last cycle of kilohertz systems as power is removed (see Fig. 8).

6. Summary

Not until the temperature drops to a suggested value of ∼2500 K will D^* form, producing an SW capable of producing an alpha. In Ar gas saturated D_2O RF experiments using FCC TF these conditions were expected to produce He^4. In Ar gas saturated H_2O RF experiments were expected to produce no He^4. And that was to a bases of comparison, and that is where the situation rests for the present. Of course, there was some D in the water used and maybe enough to produce the He^4 measured. The RF system is a non-obvious extension of Sonofusion, where a replacement of the oscillator with an RF liner amplifier of an input of 2 MHz piezo that functions as an antenna. It was tuned to a minimum RF reflection (Pref), power reflected, and a maximum admittance (Pfwd), with a standing wave ratio (SWR) of 1^+ $(P_{\mathrm{ref}}/P_{\mathrm{fwd}})^{0.5}/(1\text{-}\ (P_{\mathrm{ref}}/P_{\mathrm{fwd}})^{0.5})$ close to 1.00, where 1.00 indicates 100% signal transmitted. The object was to tune the SWR value close as possible to a value of 1.00. The standing wave often produces exotic colored patterns on TF standing wave surfaces [15] (Fig. 8).

The Acrylic reactor consisted of a 2-inch diameter tube with 0.5-inch wall and with placement for several spacing and sealing gasket adjusting the geometry of the PZT 20 mm disk piezo and TF at the bottom of the Acrylic 2-inch tube (Fig. 3). The tube extended up to 3/4 inch thick and 3 inch in diameter plate with an O-ring seal to a 1inch thick and 3-inch diameter utility ring that contained all the utility inputs and outputs. (temperature, pressure, heater, gases,

vacuum, sample vessels, etc.). To capture the experimental data the focus was on the center panel, a clock with a sweep second and all the critical measuring devices and gauges were captured in real time with an iPhone. The data can be graphed and examined after the experiment with no time limit.

A comparison was made between SW and muon systems primarily because muon fusion works. The important parameter to follow was the impulse and its rate. The impulse, ΔP, the change in momentum over a short time period were compared, $I_{\rm SW}$ and I_μ. A fast $I_{\rm sw}$ and a slow I_μ. I_μ is 10^{-8} times slower and was known to produce He^4. When using the term μ it refers to μ^- that was 207 times more massive and the same charge as the negatively charged electron. The two systems that produce He^4, one being an SW with $D^+ + e^- \rightarrow D^*$ $D^+ +$ SW$\rightarrow \alpha^+ +$ heat. The other being μ with $D_2 + \mu^- \rightarrow dd\mu^- + e^- \rightarrow \alpha^+ +$ heat and a series of small shockwaves. The impulse experiments are measured kg m/s (mv/s). $\Delta P = I = F\Delta t \sim md/t$, mass $\times$ distance/time. See Table 1

The distance, d, in meters e^- travels was a very short, $D^+ + e^- \rightarrow D^*$ in MC producing ($I_{\rm sw}$) and the distance μ^- travels is longer, the radius of molecule D_2. Where $D_2 + \mu^- \rightarrow dd\mu + e^- \rightarrow \alpha^+$. The $I_{\rm sw}$ was gaining an electron fast and the I_μ was losing an electron slow. It was so slow that the I_μ was less than $I_{\rm sw}$. It would seem that the very fast rate of the SW system that produces MS measured He^4 compares favorably to the example of the chosen muon system, a very slow rate system, that also produces He^4. The $dd\mu^-$ molecule has the small size of about 500 fm [16].

At 10 K the average free velocity was about $4\times 10^{+5}$ m/s. $(3kT/\text{kg}))^{0.5}$ m/s. In the MC model its central deuteron charge was degrading as it cooled during the 50 fs time frame. There was little activity except the mobile electron squeeze. As the system cooled the probability of an MC deuteron capturing an electron increases. And when this occurs one alpha was produced. The MC was destroyed, and TF crater debris was ejected along with one alpha. It picked up electrons, and the He4 preferred the Ar gas phase over the reactor's cavitating D_2O. A 50 ml Pyrex blub filed was quickly filled with Ar gas containing the produced helium and was sent to Claytor's laboratory for analyses.

Calorimetry of very small amounts of heat generated, a few tenths of a Kelvin, is not convincing to someone who is a skeptic about a process. It is easy to say many of the calorimetric measurements fall into an error zone and are not robust enough for as stand-alone evidence for the world sceptic. The addition measured He^4 makes for a more convincing argument for the process.

Hydrogen and its isotope ion radii, the only element that loses one electron to collapse its volume shrinks 10^{-7} times its D^* value. The muon's path as it replaces an electron with μ^- it shrinks to a volume of about 3×10^{-7} times smaller. This scale of volume change only belongs to the hydrogen isotopes and no other elements. The D^+ expansion is fast, 6×10^{-15} s and is an explosion and leads to an SW and α. On the other hand, the muon caused implosion leads to a He^4 atom. It is important to compare a μ^- system that was known to produce helium using muons and D atoms [9]. Compare that to the SW system that squeezes the MC deuterons. As the MC cools, the first and only free electron combines with deuteron forming D* atom. Where D^* combines with an electron in the MC and the SW destroys it within the debris was the alpha. In the comparison at the atomic scale of the MC and the muon impulse $I_{\rm MC}$ and $I\mu^-$, where the μ^-'s rate is $\times\ 10^{+6}\ s^{-1}$ that produces a chain He^4 atoms and the MC SW rate, in the MC, is $1.67\times 10^{+15} s^{-1}$ that produces one He^4 atom. And $I_{\rm SW}$ has a 60 times larger impulse because of its comparative high rate.

There is good data in an Ar gas environment. The temperature collisions between deuterons Ar atoms reduces the temperature system used in RF experiments that are about 3000 K the hydrogen is 100% D^+ and in the time frame of 50 fs the probability is 50% that $D^+ + e^- \rightarrow D^*$ initiating $D^+ + D^* \rightarrow \alpha$. Evaluating the three hydrogen isomers we have used D to generalize what has been discovered to help understand the H atom system. And for the tritium the measurement there was nothing above background. The positive MS He^4 results for both H and D isotopes in their RF runs shows that more information is needed for the hydrogen atom as the logical product would be D_2 not He^4. The RF experiments used more water, 80 g, of H_2O at 0.016% D is more than enough $3\times 10^{+19}$ D atoms in 80 g water more than enough to make 10^{+19} He^4.

At 10 K the average free velocity was about $4\times 10^{+5}$ m/s. $(3kT/\text{kg}))^{0.5}$ m/s. In the MC model its central deuteron charge was degrading as it cooled during the 50 fs time frame. There was little activity except the mobile electron

squeeze. As the system cooled the probability of an MC deuteron capturing an electron increases. And when this occurs one alpha was produced. The MC was destroyed, and TF crater debris was ejected along with one alpha. It picked up electrons, and the He^4 preferred the Ar gas phase over the reactor's cavitating D_2O. A 50 ml Pyrex bulb filed with Ar gas containing the produced helium was sent to Claytor's laboratory for analyses.

Hydrogen and its isotope ion radii, the only element that loses one electron to collapse its volume shrinks 10^{-7} times its D^* value. The muon's path as it replaces an electron with μ^- it shrinks to a volume of about 3×10^{-7} times smaller. This scale of volume change is about the same for all the hydrogen isotopes. The D^+ expansion is fast, 6×10^{-15} s and is an explosion and leads to a SW and α. The other an implosion leads to $\mu^-\alpha$. It is important to compare a μ^- system that was known to produce helium using muons and D atoms [9]. Compare that to the SW system that squeezes the MC deuterons. As the MC cools the first free electron combines with deuteron forming D^* atom. Where D^* combines with an MC D^+ in the debris of the destroyed MC forming the alpha. In the comparison at the atomic scale of the MC and the muon impulse $I_{\rm MC}$ and $I\mu^-$, where the μ^-'s rate is 10^{+6} s^{-1} that produces He^4 atoms and the MC SW rate, in the MC, is $1.67\times10^{+15}s^{-1}$ that produces one He^4 atom and it is finished. And $I_{\rm SW}$ has a 60 times larger impulse; lower energy but a higher rate.

Ar gas environment was a good environment for the RF experiments as the temperature collisions between deuterons and Ar atoms reduces the temperature system used in RF experiments that are about 3000 K the hydrogen is 100% D^+. What was good for H system is good for the D system. In the time frame of 50 fs the probability is 50% that $D^+ + e^- \rightarrow D^*$ initiating $D^+ + D^* \rightarrow \alpha$. Evaluating the three hydrogen isomers we have used D and H interchangeably to generalize what has been discovered to help understand the H atom system. We point out the H_2O used in RF3 H_2O Cu run, Fig. 6A, had more than enough D to make He^4 that was measured by its MS analysis. The tritium measurement there was nothing above background yet. The positive MS He4 results for both H and D isotopes in their RF runs shows that more information is needed for the hydrogen atom as the logical product would be D_2 not He^4. The RF experiments used more water, 80 g, of H_2O at 0.016% D is more than enough $3\times 10^{+19}$ D atoms to produce 10^{+15} He^4 atoms.

7. Conclusions

Reactor gases free from air that contains helium were analyzed by an MS instrument built for He^4 analysis. He^4 was found in two runs, but there were issues that troubled the MS analyses. These issues have been resolved here and the results are better than expected. The use of impulse, I, applied to a comparison of an $I_{\rm sw}$ and a muon fusion I_μ, that has a very slow path to helium production, shows that an RF $I_{\rm sw}$ path to He^4 should not be considered unusual. The RF cavitation system gave more flexibility to running our experiments and adds more knowledge to the cavitation processes that have different lattice arrangements for storing helium or ejecting it. Finding helium was a confirmation that higher frequencies, 2 MHz, maintain the energy density to produce helium as was shown in a 46 kHz system [14].

Acknowledgements

I would like to thank Dewey Weaver and Tom Darden of I.H. who supported the laboratories of Thomas Claytor; and Malcom Fowler, who were responsible for the tritium, He^4 MS measurements. Kim Nunlist who helped with the data gathering of the old systems. And Julie Wallace my wife for her patience and support.

References

[1] T.Watkins, *Rate of Proton Electron Capture*, San Jose Physics Department, San Jose , CA, 2018.

[2] Hugh G. Flynn, Method of generating energy by acoustically induced cavitation fusion and reactor therefor, US4333796A, 1982.

[3] S. Puterman, B. Braber, R. Hiller and R. Lofstedt, , Converting acoustic energy into useful other energy forms, UCLA Physics Dept., 1995.
[4] R. Stringham, Firstgate Energies, US patent 16867455, Experimentation Apparatus to Test for Heat Produced by Cavitation, 1996 and 2020.
[5] R. Stringham, Deuteron plasmas driven to neutrality and ^{4}He, *J. Condensed Matter Nucl. Sci.* **29** (2019) 22.
[6] R.S. Stringham, Conservation of E and M, single cavitation heat events, *J. Condensed Matter Nucl. Sci.* **15** (2015) 55.
[7] PTB definition: an anomalous heat production related to He^4 atom production. It is identified a $\Delta(T_2\text{-}T_1)$ added to the input energy measurement over any time length.
[8] T. Claytor and M. Fowler, Development of a sensitive system for the measurement of trace amounts of He^4 in deuterium or hydrogen, *ICCF 21 proceedings*, Fort Collins, CO USA, 3–8 June (2018) (1994).
[9] K. Nagamine, *Introductory Muon Science*, Cambridge University Press, Cambridge, 2003, p. 78.
[10] N. Lawandy, Interactions of charged particles on surfaces, *Appl. Phys. Lett.* **95** (2009) 234101.
[11] T. Weidman, Special Relativity and Thermal/Statistical Physics 9HB, UC Davis, 2019.
[12] P. Pagano, A, Bemporad and D.H. Mackay, Hydrogen non-equilibrium ionization effect in coronal ejections, A&A 637,A49, **639** (2020).
[13] S. BenZvi, The mean lifetime of the muon, Department of Astro Physics. U. of Rochester, 2018.
[14] R. Stringham, Helium measurements from target foils, LANL and PNNL 1994, *J. Condensed Matter Nucl. Sci.* (2017).
[15] R. Stringham, Sonofusion produces tritium that decays to He^3, 15th ICCF, CMNS, Rome, Italy, Oct. 5–9, 2009, pp. 57.
[16] D.V. Balin, V.A. Ganzha, S M. Koslov, E.M. Maev, G.V. Petrov and M.A. Soroka, High precision study of muon fusion in D_2 and HD gas, Russia, Switerland, Austria, USA, and Germany**,** Russian Federation N$^{\text{O}}$ HIII-3057.2006.2, in part by the Russian Foundation of Fundamental Research (grants N$^{\text{O}}$ 00−15−96813 and N$^{\text{O}}$ 08−02−00055), by the Russian Ministry of Sciences and Technology, by the Paul Scherrer Institute, by the Austrian Academy of Sciences and by the US Department of Energy, 2009.